**ORIGINAL PAPER**

# EGCG attenuate EGF triggered matrix abundance and migration in HPV positive and HPV negative cervical cancer cells

Rajalakshmi Sabanayagam[1] · Sneha Krishnamoorthy[1] · Jayapradha Gnanagurusamy[1] · Bharathi Muruganatham[2] · Sridhar Muthusami[1,2]

## Abstract

Our previous laboratory findings suggested the beneficial effects of epigallocatechin gallate (EGCG) against cervical cancer (CC) cells survival. The present study is aimed at identifying the effects of EGCG in preventing the actions of epidermal growth factor (EGF) in human papilloma virus (HPV) 68 positive ME180 and HPV negative C33A CC cells. An elevated level of EGF in tumor micro-environment (TME) is linked to the metastasis of several cancers including CC. We hypothesized that EGCG has the ability to block the actions of EGF. To test this, survival assay was performed in cells treated with or without EGF and EGCG. The mitochondrial activity of cells was ascertained using MTT assay and mitored staining. Protein and non-protein components in the extracellular matrix such as collagen and sulphated glycosaminoglycans (GAGs) were evaluated using sirius red and alcian blue staining, respectively. Matrix metalloproteinase-2 (MMP-2) gene expression and enzymatic activity were assessed using real time-reverse transcriptase-polymerase chain reaction (RT-PCR) and gelatin zymography. Wound healing assay was performed to assess the EGF induced migratory ability and its inhibition by EGCG pre-treatment. Clonogenic assay showed that EGCG pre-treatment blocked the EGF driven colony formation. In silico analysis performed identified the efficacy of EGCG in binding with different domains of EGF receptor (EGFR). EGCG pre-treatment prevented the epithelial–mesenchymal transition (EMT) and metabolic activity induced by EGF, this is associated with concomitant reduction in the gene expression and enzyme activity of MMP-2. Further, reduced migration and ability to form colonies were observed in EGCG pre-treated cells when stimulated with EGF. HPV positive ME180 cells showed increased migratory and clonogenic ability upon EGF stimulation, whose effects were not much significant in HPV negative C33A cells. EGCG effectively blocked the actions of EGF in both HPV positive and HPV negative conditions and can be advocated as supplementary therapy for the management of EGF driven CC. However, further studies using cell line-derived xenograft (CDX)/patient-derived xenograft (PDX) model system is warranted to validate the therapeutic utility of EGCG.

✉ Sridhar Muthusami
   sridharuniv@gmail.com; sridhar.m@kahedu.edu.in

1   Department of Biochemistry, Karpagam Academy of Higher Education, Coimbatore, Tamil Nadu 641021, India

2   Karpagam Cancer Research Centre, Karpagam Academy of Higher Education, Coimbatore, Tamil Nadu 641021, India

## Graphical abstract
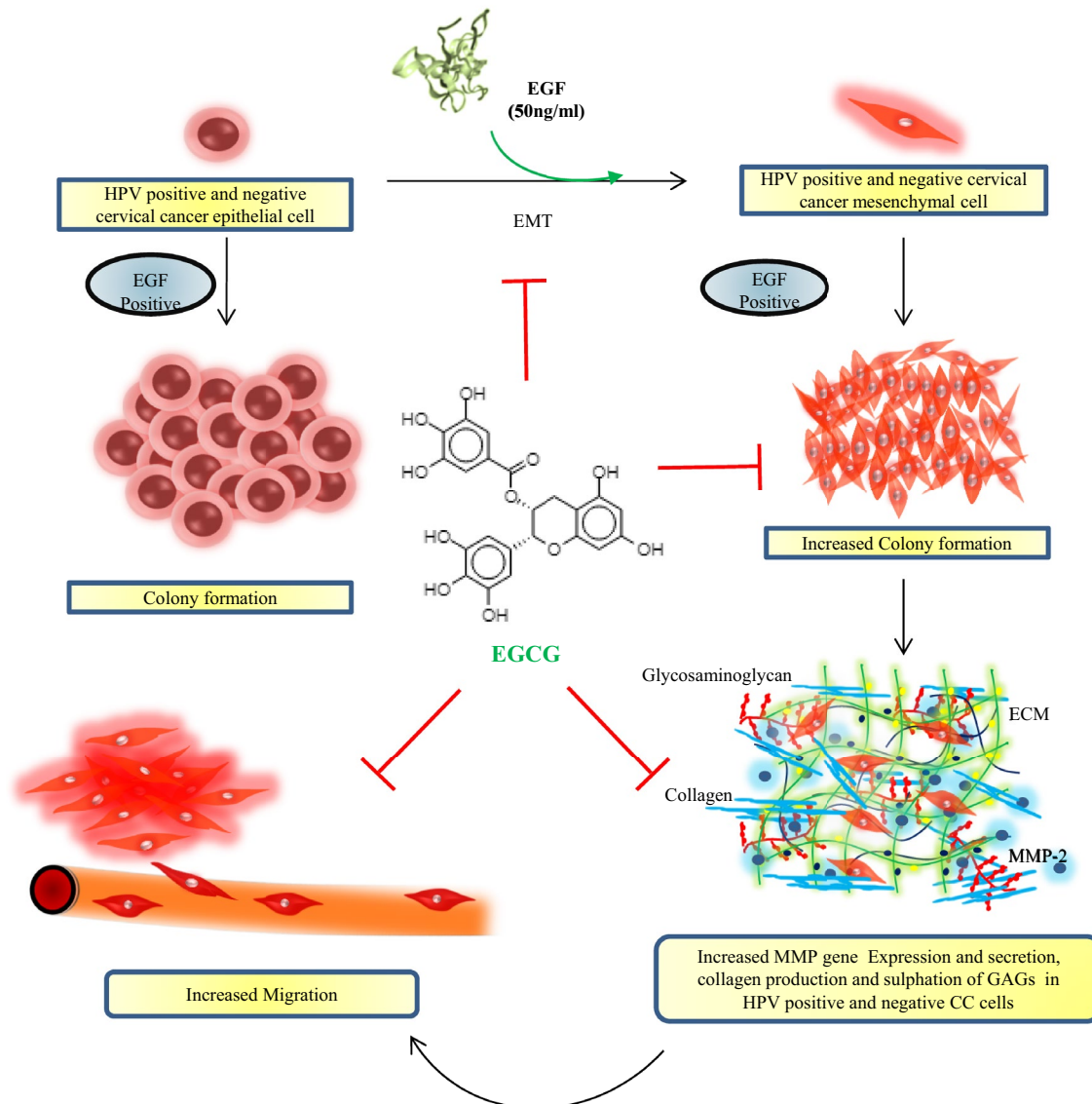


**Keywords** EGCG · EGF · MMP-2 · ECM · Migration · TKI

## Abbreviations

| | | | |
|---|---|---|---|
| ANOVA | Analysis of variance | EMT | Epithelial-to-mesenchymal transition |
| BE | Binding energy | FBS | Fetal bovine serum |
| CC | Cervical cancer | GAG | Glycosaminoglycan |
| CDX | Cell line derived xenograft | HIF1 | Hypoxia inducible factor 1 |
| DFS | Disease free survival | HPV | Human papilloma virus |
| DMEM | Dulbecco's Modified Eagle Medium | HSPG | Heparan sulphate proteoglycan |
| EGCG | Epigallocatechin gallate | mAbs | Monoclonal antibodies |
| EGF | Epidermal growth factor | miRNAs | Micro RNAs |
| EGFR | EGF receptor | MMP-2 | Matrix metalloproteinase -2 |
| | | NCCS | National Centre for Cell Sciences |

| OS | Overall survival |
|---|---|
| PDX | Patient- derived xenograft |
| RT-PCR | Real time-reverse transcriptase-polymerase chain reaction |
| TGF β | Transforming growth factor beta |
| TKI | Tyrosine kinase inhibitor |
| TKRU | Tyrosine kinase regulatory unit |
| TME | Tumor micro-environment |
| TMJM | Trans membrane juxta membrane |
| VEGF | Vascular endothelial growth factor |
| 3D | Three-dimensional |

# Introduction

An increase in the incidence of CC among developing countries is a major cause for concern. Though HPV infection is regarded as a responsible factor for the development, sustenance and progression of CC, role of EGFR is obvious [1]. Phosphorylation of EGFR at tyrosine residue 1068 is considered crucial for the initiation and propagation of EGF signaling leading to CC progression [2, 3]. A number of strategies are being used to block the actions of EGFR which include tyrosine kinase inhibitors (TKIs) and monoclonal antibodies (mAbs) [4, 5]. However, resistance to known treatments such as chemotherapy and radiotherapy are associated with constitutive expression of EGFR signaling molecule. Earlier, we have consolidated the TKIs for the treatment of CC and emphasized the need for the development of newer TKIs [1]. Consumption of green tea is associated with reduced incidence of various cancers including CC [6, 7]. Therefore, newer drugs are aimed at preventing the expression pattern of EGFR and/or controlling its phosphorylation, thereby controlling CC progression. EGCG, a flavonoid from green tea is reported to exert number of beneficial effects in treating CC. The derivatives of EGCG inhibited E7 induced cervical carcinogenesis as determined through structured dynamic observations. The oncoproteins E6 and E7 are known to increase the inhibition of the transcriptional activity and degradation of p53 and pRb, respectively [8]. Previously, we reported the ability of EGCG to increase the transcriptional activity of p53 and reduce CC cell viability [9]. A crucial role for EGF in promoting the migration of CC cells is well documented. Very recently, we reviewed the significance of EGFR targeting to improve the therapeutic outcome in CC [1].

Number of phyto-components is known to exert cytotoxicity along with the inhibition of EGFR expression in CC cells [10, 11]. The ability of EGCG to sensitize cisplatin resistance is reported [12]. Very recently, EGCG is identified to prevent EMT induced by transforming growth factor beta (TGF β) in CC HeLa and SiHa cells [13]. The consolidated actions of EGCG is known to involve the inhibition of

several molecular signaling such as EGFR, TGF β, vascular endothelial growth factor (VEGF) and hypoxia inducible factor (HIF1) signaling [14]. Several micro RNAs (miR-NAs) expressed in HPV infected CC cells are differently regulated by EGCG leading to growth inhibition [15]. The tumor architecture is highly supported by the complex matrix production and remodeling [16]. Extracellular matrix environment is known to possess the receptor for HPV, heparan sulphate proteoglycan (HSPG) which is a sulphated GAG. Similarly, Cruz and Meyers [17] revealed that HPV driven CC is highly dependent on cell surface GAGs. CC progression was reported to be associated with increased collagen accumulation and poor overall survival (OS) [18]. An isoform of collagen prolyl 4-hydroxylase, P4HA2 was identified to increase CC tumorigenesis and migration [19]. Chen et al. [20] reported that overexpression of MMPs are highly associated with the poor OS and disease-free survival (DFS) in CC patients. Meanwhile, MMP-2 expression during CC increased the disease complexity and aids in CC migration [21]. All together, it is suspected that a complexity in the tumor matrix prevents the entry of drugs for a potential treatment during CC. Collectively these observations prompted us to explore the beneficial effects of EGCG during EGF induced EMT and migration in ME180 and C33A CC cells. The current study is an attempt to verify whether EGCG pre-treatment could prevent the EGF induced matrix abundance, migration and clonogenesis of HPV positive and HPV negative CC cells.

# Materials and methods

## Cell line procurement and maintenance

HPV 68 positive ME180 and HPV negative C33A CC cells were procured from National Centre for Cell Sciences (NCCS), Pune. HPV status of the cells was authenticated using real time PCR analysis. Cells were grown in Dulbecco's Modified Eagle Medium (DMEM) with 10% Fetal Bovine Serum (FBS) media, maintained in 5% $CO_2$ incubator at 37 °C. EGCG was purchased from Sigma. EGF and other cell culture materials were purchased from Himedia.

## Induction of EMT and assessment of cell viability

$1 \times 10^4$ ME180 and C33A CC cells were seeded in a 96-well plate and were allowed to attach. It was followed by starvation for 4 h and cells with serum-free media served as control. The cells were stimulated with EGF (50 ng/ml) alone and EGCG (50 μM) alone for 24 h. To ascertain the effect of EGCG during EGF stimulated conditions, the cells were pre-treated with EGCG for 30 min with subsequent EGF stimulation for 24 h. The changes in the morphology of ME180
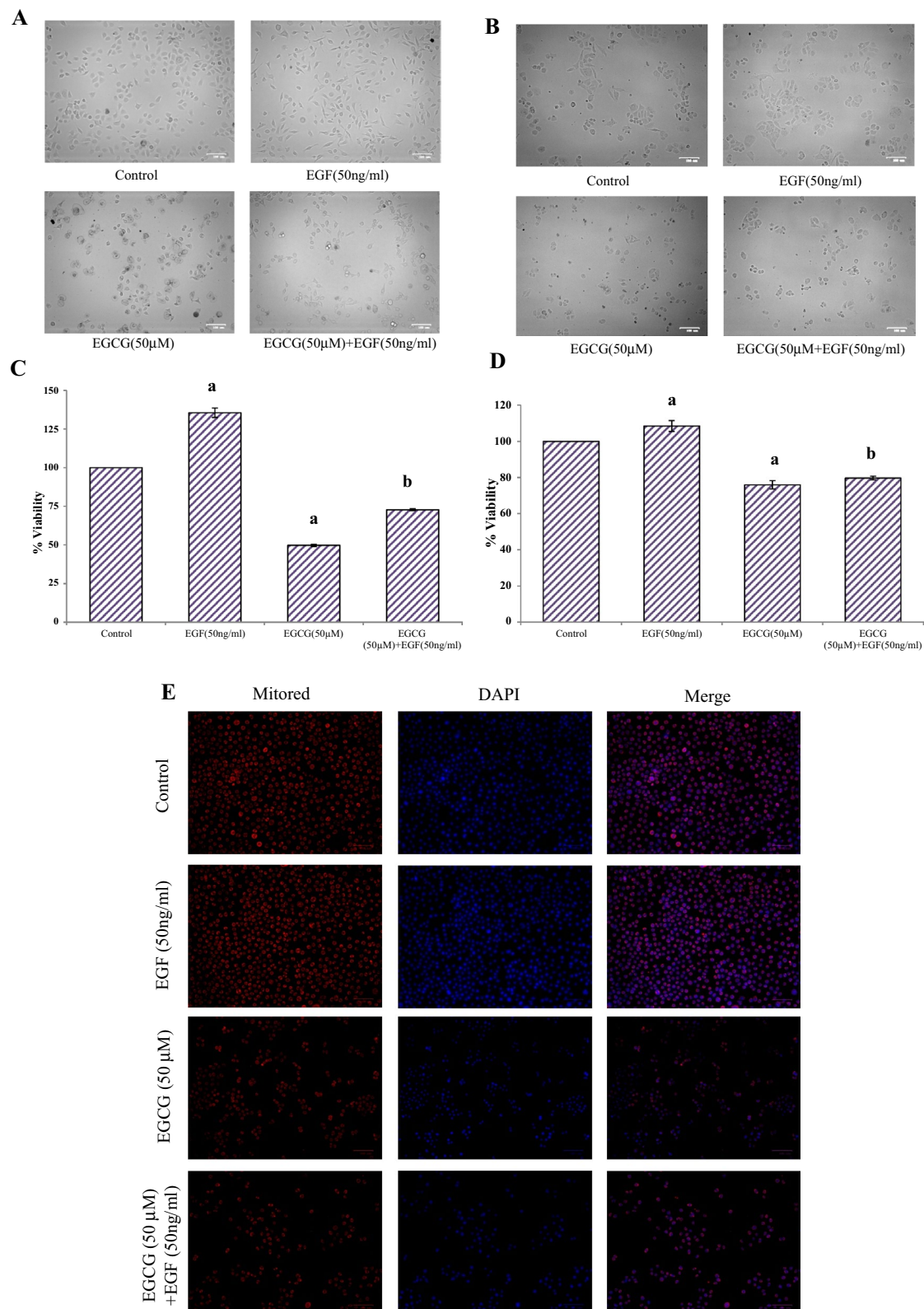
**Fig. 1** Photo-micrographs of ME180 (**A**) and C33A (**B**) cells treated with EGF demonstrate EMT changes in ME180 cells as indicated by spheroid to spindle morphology after 24 h. EGCG treatment alone has reduced the cell survival after 24 h of treatment and EGCG pre-treatment inhibited EGF induced actions in ME180 and C33A cells (*Scale* 100 μm). The graphical representation indicates the percentage viability of ME180 (**C**) and C33A cells (**D**) obtained by MTT assay. Representative fluorescent microscopy images depicting the enhanced mitochondrial membrane potential after 24 h of treatment with EGF. EGCG treatment with or without EGF stimulation displayed a reduction in the fluorescence intensity indicating reduced mitochondrial membrane potential in ME180 (**E**) and C33A cells (**F**)
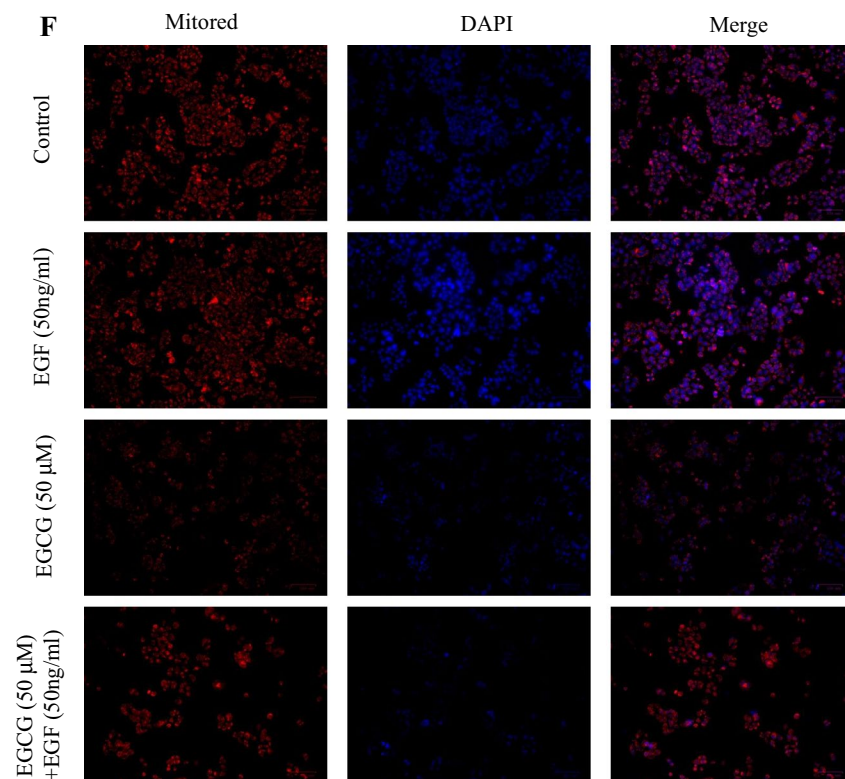
**Fig. 1** (continued)

and C33A cells were captured using Biorad ZOE fluorescent cell imager. Later on, the conditioned media was removed and MTT (0.5 mg/ml) was added to each well and were allowed to incubate for 3 h. DMSO was utilized to dissolve the formazan crystals developed and were read at 590 nm in ELISA reader (BioTek, Synergy H1). The readings obtained were plotted in a graph and represented as % viability [9].

## Assessment of mitochondrial membrane potential

The ability of EGCG to prevent the mitochondrial metabolic activity under basal and EGF stimulated condition in ME180 and C33A cells were ascertained. Briefly, $5 \times 10^3$ cells were seeded in 96 well plates and were allowed to attach. The cells were treated as described in the previous "Induction of EMT and assessment of cell viability" section. After 24 h of treatment time, the regulatory role of EGCG on EGF stimulated mitochondrial membrane potential was ascertained. The cells were washed with PBS and 200 nM mitored (Sigma-Aldrich-53271) was added to each well and were allowed to incubate for 30 min. The cells were then counterstained with DAPI and the photo-micrographs were captured immediately using a fluorescent cell imager.

## Assessment of collagen deposition

The cells were seeded in 24 well plates and treated as per "Induction of EMT and assessment of cell viability" section. After 24 h, the conditioned media were removed and the cells were washed with PBS. Further, it was allowed to fix using 70% ethanol for 1 h. 0.1 g sirius red was dissolved in saturated picric acid solution which was added to each well and incubated overnight. After incubation, the cells were washed with distilled water until the unbound dyes were removed. The photo-micrographs were taken using an inverted microscope and quantified at 490 nm in ELISA reader upon dissolving the dye in 1 M NaOH [22].

## Assessment of sulfated GAGs

The cells were seeded in a 24-well plate and treated as per "Induction of EMT and assessment of cell viability" section. After 24 h, the cells were subjected to PBS wash and fixed using 2% glacial acetic acid for 1 h. The cells were rinsed using 95% and 70% ethanol, followed by addition of 0.5% alcian blue stain and incubated overnight. The unbound dyes were washed using 0.1 N HCl and distilled water. The photo-micrographs were captured and the intensity of dye was quantified using 6 M guanidine HCl solution at 600 nm using ELISA reader [23].
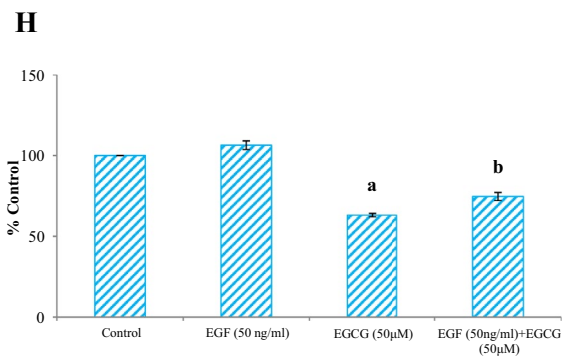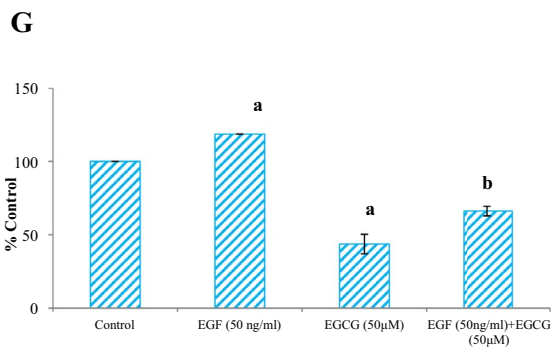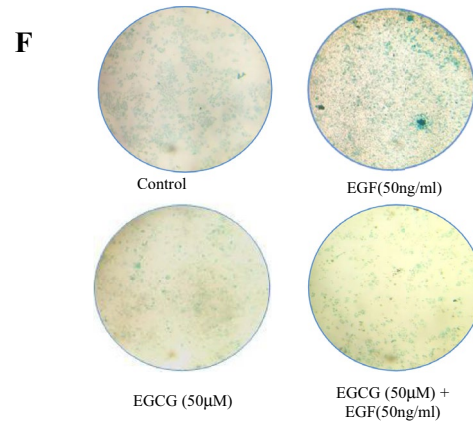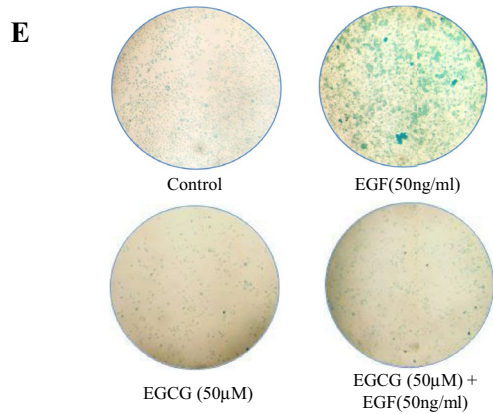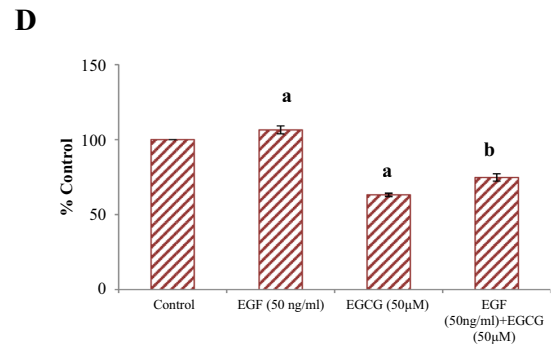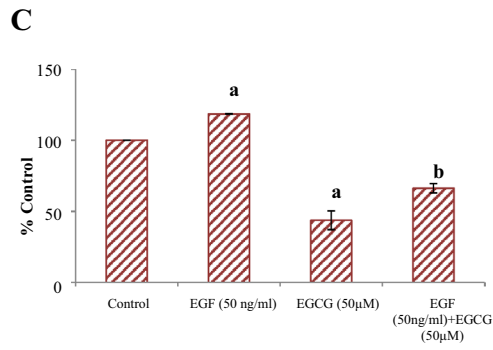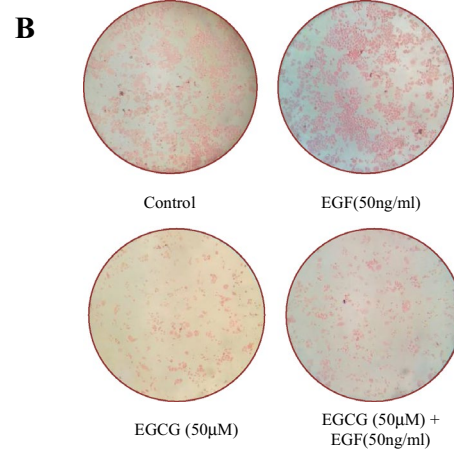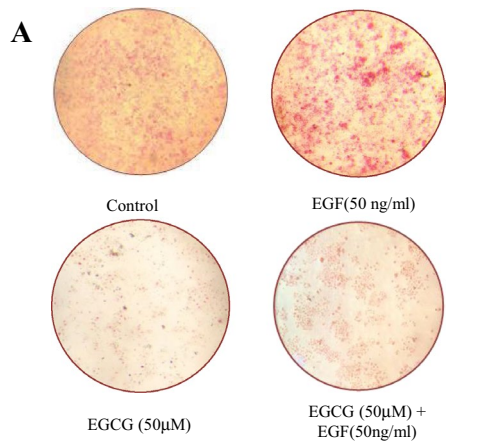
◀**Fig. 2** The photo-micrographs denotes the intensity of the collagen deposition in ME180 (**A**) and C33A cells (**B**) as identified by sirius red staining. The stain intensity in ME180 (**C**) and C33A cells (**D**) was quantified at 490 nm and represented graphically. Further, the photo-micrographs denote the amount of sulphated GAGs deposition in ME180 (**E**) and C33A cells (**F**) as identified by alcian blue staining. The stain intensity in ME180 (**G**) and C33A cells (**H**) was quantified at 600 nm and represented graphically.

## RT-PCR analysis

ME180 cells were treated as described in the previous "Induction of EMT and assessment of cell viability" section. After 24 h, the cells were washed with ice cold PBS. TRIzol was added to each plates and were placed on rocker for 10 min. Then the cell lysate was collected and stored at −80 °C until RNA extraction. RNA extraction was done using the method previously described [24]. RNA with purity from 1.6 to 1.9 was subjected to cDNA synthesis (GBiosciences). RT-PCR was performed using EvaGreen qPCR Master Mix (GBiosciences) and specific primers for MMP-2 (Forward primer—5′-GATACCCCTTTGACGGTA AGGA-3′ and reverse primer—5′-CCTTCTCCCAAGGTC CATAGC-3′). β-Actin gene was simultaneously amplified using specific primers (Forward primer—5′-GACAGGATG CAGAAGGAGATCACT-3′ and reverse primer—5′-TGA TCCACATCTGCTGGAAGGT-3′) and the fold changes were calculated using the formulae $2^{-\Delta\Delta C_t}$ [23].

## Zymography analysis

The cells were treated as described earlier in "Induction of EMT and assessment of cell viability" section. The conditioned medium was collected and spun at 1000 RPM for 5 min to remove the cell debris. The supernatant was transferred to a new tube and lyophilized (BORG Lyo4). The concentrated conditioned media was reconstituted in a lower volume to achieve 20× concentration. After estimating the protein concentration, equal amount of proteins were electro-separated in a SDS gel containing 1% gelatin, a substrate for MMP-2. After separation, the gel was placed in a renaturation buffer for 18 h and stained using Coomassie brilliant blue. Areas of MMP-2 activity were visualized as white bands in a blue background after destaining. The white band developed was captured and documented using Chemidoc Biorad [10].

## Wound healing assay

ME180 and C33A cells were seeded in a 6 well plate and maintained in 5% $CO_2$ incubator at 37 °C. After confluency, a wound was created evenly in all wells using sterile 200 µl pipette tip and the scratched cells were removed by gentle washing with PBS. The cells were treated as described earlier in "Induction of EMT and assessment of cell viability" section at indicated time points. Images were captured and recorded at 0 h, 12 h, 24 h and 36 h intervals for ME180 cells and 0h, 24h, 36h and 48h intervals for C33A cells using fluorescent cell imager to analyze the effect of EGCG on inhibiting the EGF induced migratory ability [3].

## Clonogenic assay

The ME180 and C33A cells were plated in 12 well plate with 800 cells/well and maintained at 37 °C in 5% $CO_2$ incubator. The treatment groups are same as mentioned in previous "Induction of EMT and assessment of cell viability" section. After 24 h, the treated cells were replaced with 2% serum media for 7 days. Then the cells were washed with PBS, fixed with ice cold methanol and stained using 0.05% crystal violet and the colonies were counted and plotted in a graph [23].

## Molecular docking

The chemical three-dimensional (3D) structure of EGCG was obtained from the database of PubChem compounds in sdf format. The EGFR domains were retrieved from PDB as 6duk. All the domains in PDB format and EGCG were converted into PDBQT file using PyRx tool with an option Auto dock Vina v1.1.2 for docking. We used UFF force field and conjugate gradients as an optimization algorithm with 200 steps in this molecular docking. EGCG was evaluated using the Mol inspiration property calculator (http://www.molinspiration.com/) to identify drug-likeness and bioactivity prediction [25].

## Statistical analysis

The statistical analysis performed in this study utilized analysis of variance (ANOVA) to evaluate the numerical data generated. The Student "*t*" test was used to determine the variations among each group using numerical data from at least three independent, consecutive triplicates. If $p \leq 0.05$, it is considered statistically significant.

## Results

### EGCG pre-treatment prevented the EGF induced viability and mitochondrial membrane potential

The growth inhibitory actions of EGCG and growth promoting effect of EGF were known [3, 9]. Here, we sought to identify the inhibitory effects of EGCG in HPV positive
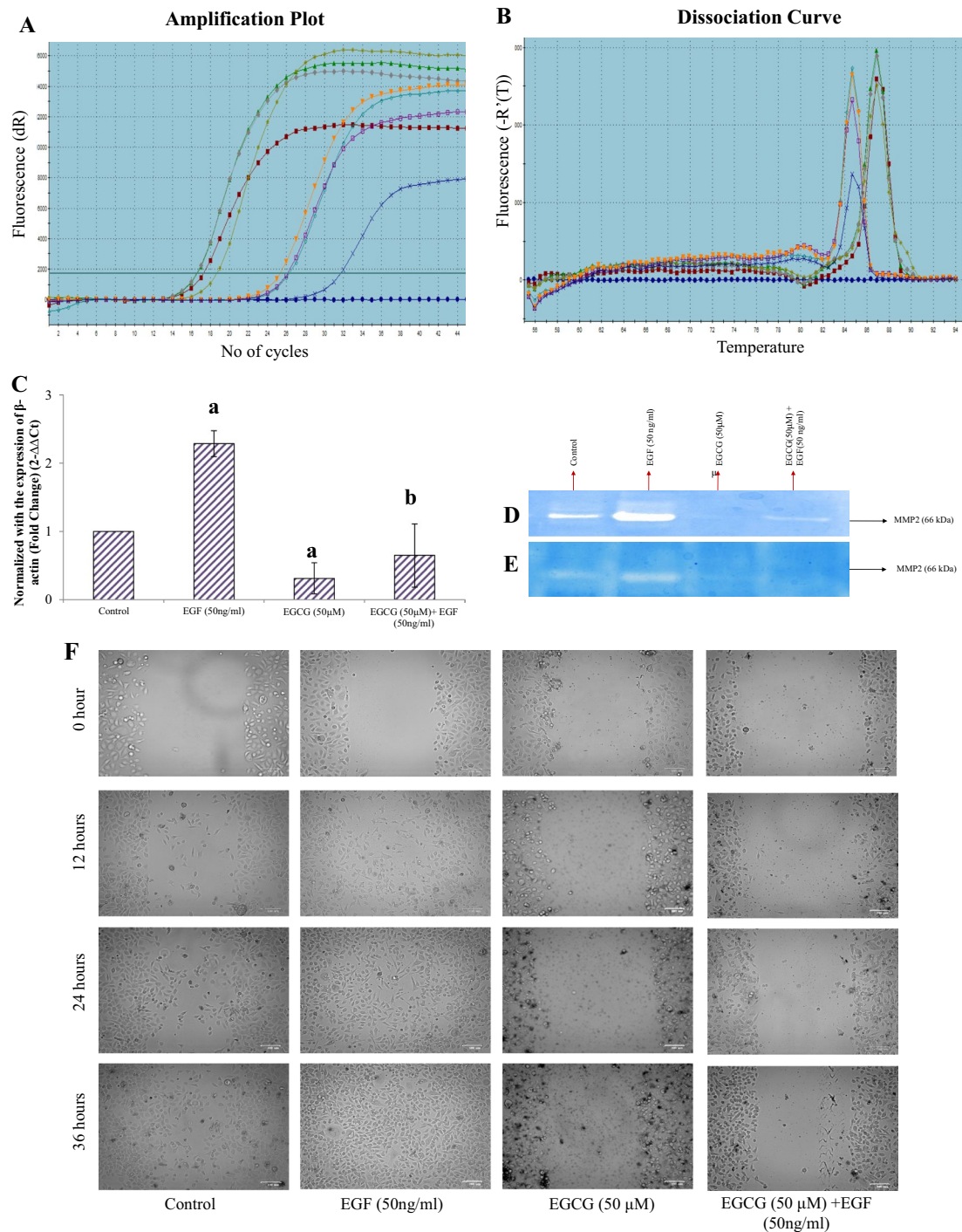
**Fig. 3** The amplification plot (**A**) and dissociation curve (**B**) obtained for the MMP-2 gene expression and the fold change were represented in the graph (**C**). Alphabet 'a' indicates statistical significance when compared with control at $p \leq 0.05$ and alphabet 'b' indicates statistical significance when compared with EGF at $p \leq 0.05$. Representative zymogram depicting the activity of the MMP-2 enzyme in the conditioned medium of ME180 cells (**D**) and C33A cells (**E**) as indicated by white bands. The intensity of the band indicates higher MMP-2 activity in EGF treatment. EGCG treatment with or without EGF stimulation displayed a reduction in the MMP-2 activity. Photomicrographs of scratch healing assay performed in ME180 cells (**F**) and C33A cells (**G**) at indicated time points. Treatment with EGF demonstrates increased migratory ability in a time dependent manner. EGCG treatment with or without EGF stimulation reduced the migratory ability of ME180 and C33A cells. Photo-micrographs of plates showing the ability of ME180 cells (**H**) and C33A cells (**I**) to form colonies. EGF treatment increased the number of colonies in ME180 cells. EGCG alone/pre-treatment before EGF stimulation inhibited the clonogenesis. The colonies were counted manually and represented in the graph plotted. Alphabet 'a' indicates statistical significance when compared with control at $p \leq 0.05$ and alphabet 'b' indicates statistical significance when compared with EGF at $p \leq 0.05$.
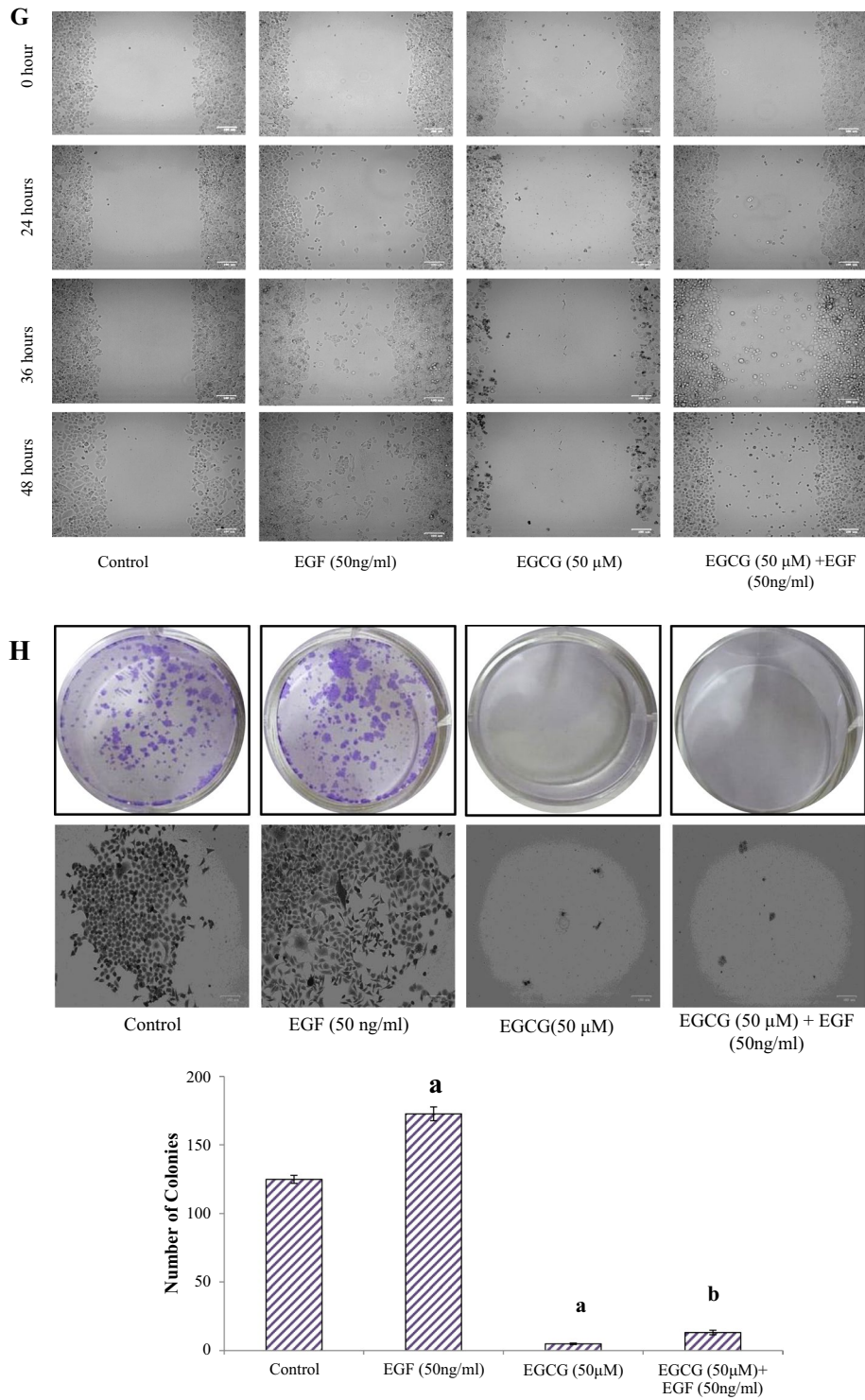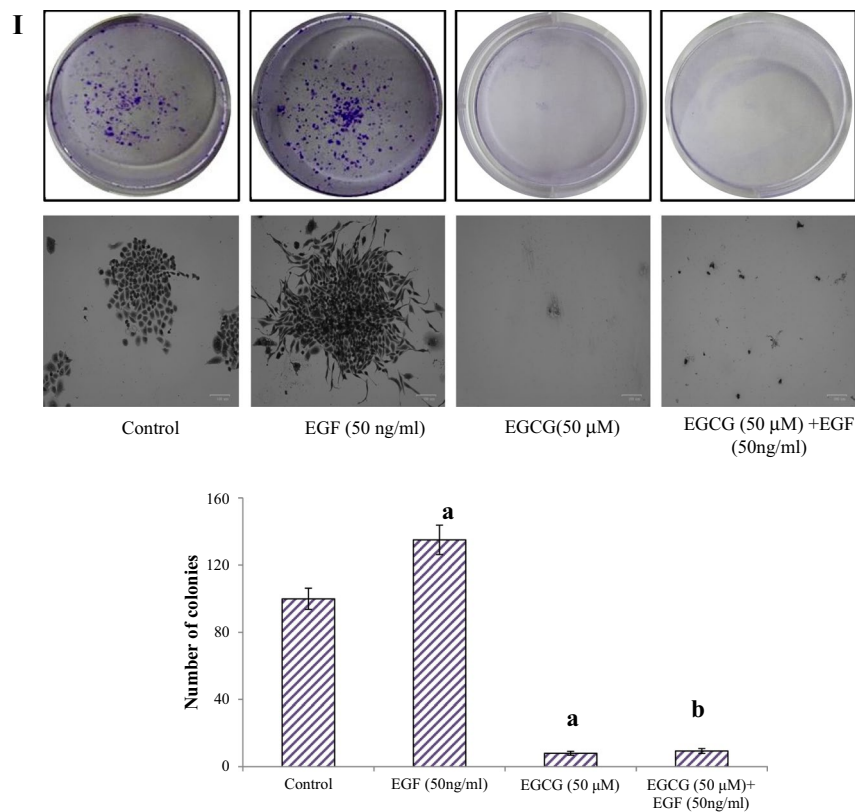
**G**



**H**



Control    EGF (50 ng/ml)    EGCG(50 μM)    EGCG (50 μM) + EGF (50ng/ml)



**Fig. 3** (continued)

**Fig. 3** (continued)

ME180 and HPV negative C33A cells. To stimulate EGF rich micro-environment, ME180 and C33A cells were left treated or untreated with EGF (50 ng/ml). The concentration of EGF is chosen based on our previous data [3]. To assess the ability of EGCG in preventing EGF induced EMT, the cells were pre-treated with EGCG for 30 min, before stimulating with EGF. Photo-micrographs of the cells were captured at the end of treatment time that showed EMT in EGF treated ME180 cells. Interestingly EGF failed to induce EMT in cells pretreated with EGCG in ME180 (Fig. 1A) and C33A cells (Fig. 1B). The percentage viability obtained indicates the significant increase in EGF induced viability and the inhibitory actions of EGCG in EGF stimulated ME180 (Fig. 1C) and C33A cells (Fig. 1D). Mitored stains the cellular mitochondria based on their mitochondrial membrane potential and the intensity of the stain is directly proportional to the mitochondrial activity. Therefore, mitored counterstained with DAPI was performed to evaluate the mitochondrial membrane potential which in turn is an index of the energy reservoir of the cells. Thus, upon staining, the mitochondrial membrane potential was captured and documented using fluorescent microscopy. EGF treatment showed the increased fluorescence signifying the elevated mitochondrial activity, which is decreased upon EGCG pre-treatment (Fig. 1C, D).

## EGCG pre-treatment prevented the deposition of matrix components

The increased accumulation of protein and non-protein components in extracellular matrix is an indicative of resistance towards drug entry. An attempt was made to identify the regulatory role of EGCG in tumor region, for which Sirius red staining was employed to detect the collagen deposition in both the cell lines (Fig. 2A–D). Similarly, sulphated GAGs were detected using alcian blue staining at pH 2.5 (Fig. 2E, H). EGF stimulated cells exhibited increased staining intensity when compared with control. EGCG alone or EGCG pre-treated cells showed relatively less staining intensity. This indicates that EGCG pre-treatment prevents the deposition of collagen and sulphated GAGs, a crucial component for the matrix complexity.

## EGCG pre-treatment prevented EGF induced mRNA expression, enzyme activity of MMP-2 and wound healing

In order to understand the relevance of inhibitory effects of EGCG upon EGF stimulation, the expression pattern of MMP-2 were evaluated. An increase in the abundance of MMP-2 gene expression after 24 h stimulation with EGF is consistent with our previous findings. EGCG pre-treated cells did not display abundance of these transcripts as evidenced by RT-PCR analysis. A number of transcription factors that are activated by EGF are known to enhance the expression of MMP-2. It will be interesting to evaluate the effect of EGCG pre-treatment and the availability of these transcription factors to understand the molecular mechanism of EGCG. Nevertheless, the present study clearly document the ability of EGCG in preventing the EGF induced mRNA expression of MMP-2 in ME180 cells (Fig. 3A–C). To understand the functional relevance of enhanced EMT upon EGCG treatment, we sought to evaluate the enzyme activity of MMP-2 in basal and EGF stimulated cells. For this, the conditioned media were concentrated upto $20\times$. The equal amount of total proteins was resolved in a gel embedded with 1% gelatin and the enzyme activity was assessed by the digestion of gelatin by MMP-2. The intensity of the band was abundantly increased in the EGF treated group when compared with control. EGCG treated group exhibited very low amount of MMP-2 activity. EGCG pre-treatment prevented the MMP-2 activity induced by EGF stimulation. Thus the zymogram analysis documents the inhibitory effects of EGCG towards the MMP-2 enzyme activity in both HPV positive ME180 and HPV negative C33A cells (Fig. 3D, E).

To address the functional relevance of EGF induced EMT and ability of EGCG to prevent this transition, we analyzed the role of EGCG in inhibiting the EGF induced migration. This was ascertained using a wound healing assay, which utilize the ability of cells to migrate towards the wound created. Wound healing was assessed at different time points such as 0 h, 12 h, 24 h and 36 h in ME180 cells and 0h, 24h, 36h and 48h in C33A cells. EGF treatment has resulted in complete closure of wound after 36 h of treatment; however EGCG pre-treatment for 30 min prevented the EGF induced migration in ME180 cells (Fig. 3F). This reduction could be a consequence of impaired MMP-2 gene expression and enzyme activity as evidence by RT-PCR and zymography analysis, respectively. EGF induced less significant migratory ability in C33A cells and wound closure than ME180 cells. However EGCG pre-treatment for 30 min prevented the EGF induced migration in C33A cells and ME180 cells indicating the efficacy of EGCG in HPV positive and negative CC cells (Fig. 3G).

## EGCG has the ability to prevent the formation of colonies as assessed by clonogenic assay

The present study shows an increase in number of clones after stimulation with EGF in ME180 and C33A cells. This suggests the ability of EGF to form colonies, an index of tumor relapse. Interestingly, pre-treating the cells for 30 min with EGCG and subsequent stimulation with EGF failed to increase the number of colonies. This is the first study to show the ability of EGCG in attenuating EGF driven clonogenesis in both ME180 and C33A cells (Fig. 3H, I). This data also supports an earlier observation by Sharma et al. [26] where in they showed the ability of EGCG to prevent CC cell proliferation.

## EGCG has the ability to bind to the catalytic domain of EGFR as assessed by in silico analysis

To validate the in vitro findings, we performed computational analysis. Docking studies were conducted to identify putative amino acids that are involved in the interaction between EGFR and EGCG. To evaluate the comparative efficacy of EGCG, gefitinib was used as positive control to dock with EGFR. The docking studies revealed a better binding ability of EGCG than gefitinib. The EGCG interacted well with the EGFR domain I and II and the binding energy (BE) was observed as $-7.0$ kcal/mol with the RMSD value of 1.386 Å. The EGCG formed the two conventional hydrogen bonds with the residues THR266 and GLU60 and formed the pi alkyl and alkyl bond with the residues VAL6 and VAL36. Also, the pi cation formed with the residue LYS4. However, the BE for the gefitinib interacted with the EGFR domain I and II (BE = $-6.5$ kcal/mol; RMSD = 3.457 Å) was observed low when compared with the EGCG (Fig. 4A).

The EGCG interacted significantly with the EGFR domain III and IV and the BE was noted as $-9.0$ kcal/mol with the RMSD value of 0.137 Å. The EGCG formed the five conventional hydrogen bonds with the residues LYS455, PRO496, SER501, CYS502, SER506, and SER529. Likewise, the EGCG interacted with the residue LYS430 and VAL500 by using the pi-alkyl and alkyl bonds. The gefitinib formed the carbon-hydrogen* and conventional hydrogen bond with the residues LEU518*, GLU519*, and ALA542 with the BE of $-6.0$ kcal/mol, and the RMSD was noted as 4.158 Å. Also, the residues such as interacted CYC515, LEU539, and PRO540 interacted with gefitinib using the pi alkyl and alkyl bond. The halogen bond is formed with the residues PRO536 and CYS538 (Fig. 4B).

The EGCG interacted well with the EGFR tyrosine kinase regulatory unit (TKRU) with the BE of $-7.6$ kcal/mol and the RMSD was observed as 0.137 Å and the residues TRP731 and GLN791 interacted with the EGCG using pi-stacked and conventional hydrogen bond. However, the gefitinib

**Fig. 4** The docking pose of the EGFR domains I and II with the EGCG and gefitinib based on the binding affinity and interacting residues (i, iii). The type of bonds involved in interacting EGCG and gefitinib with domains I and II residues (ii, iv) (**A**). The docking pose of the EGFR domains III and IV with the EGCG and gefitinib based on the binding affinity and interacting residues (v, vii). The type of bonds involved in interacting EGCG and gefitinib with domains I and II residues (vi, viii) (**B**). The docking pose of the EGFR TKRU domains with the EGCG and gefitinib based on the binding affinity and interacting residues (ix, xi). The type of bonds involved in interacting 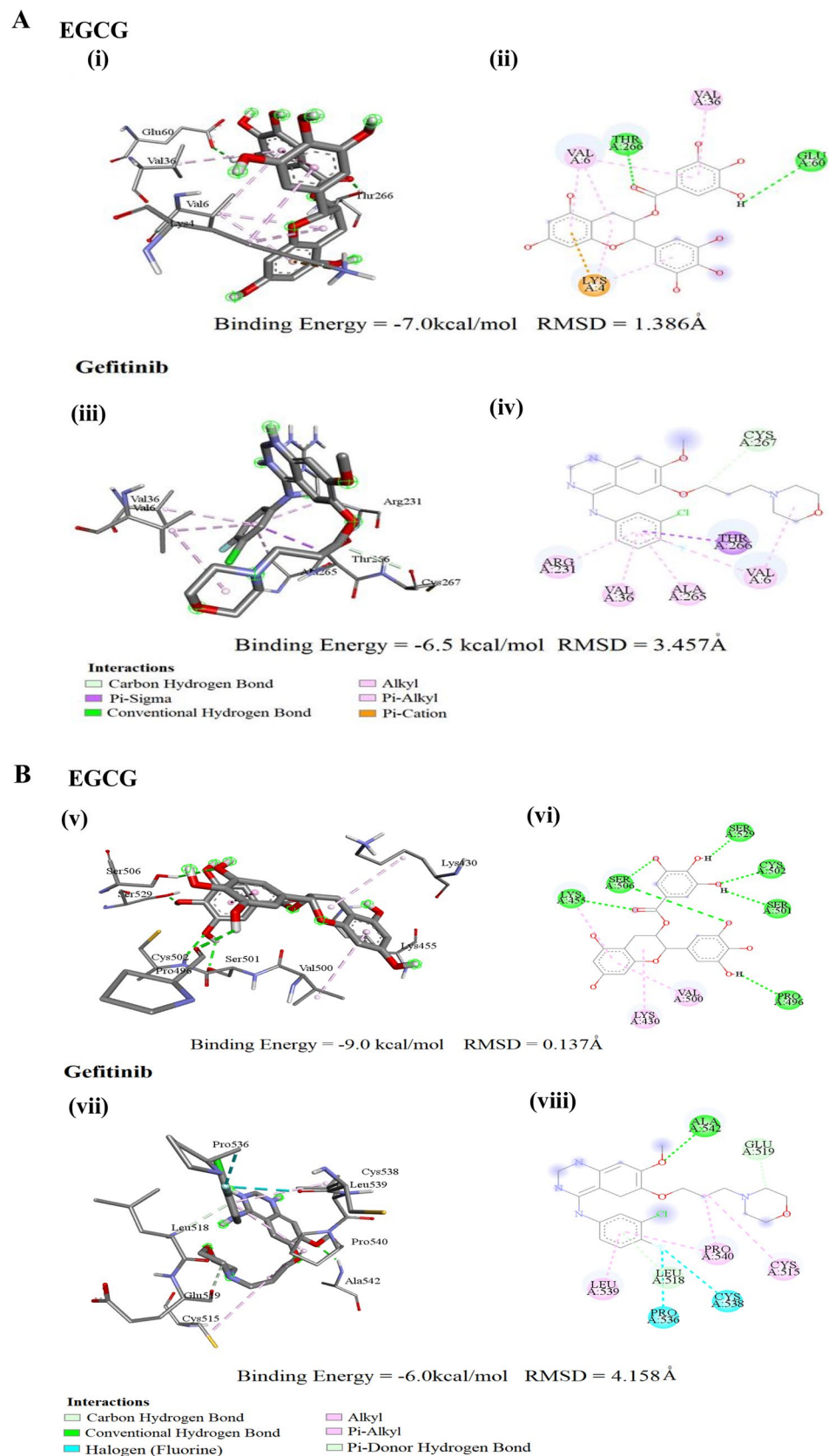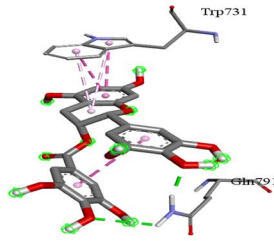EGCG and gefitinib with domains I and II residues (x, xii) (**C**). The docking pose of the EGFR TMJM domains with the EGCG and gefitinib based on the binding affinity and interacting residues (xiii, xv). The type of bonds involved in interacting EGCG and gefitinib with domains I and II residues (xiv, xvi) (**D**).
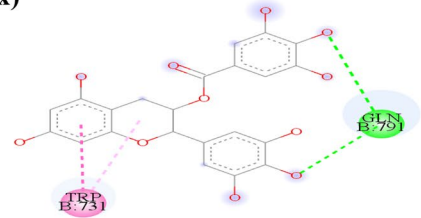
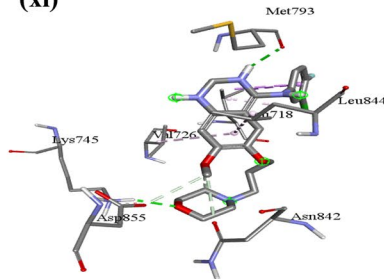**Fig. 4** (continued)
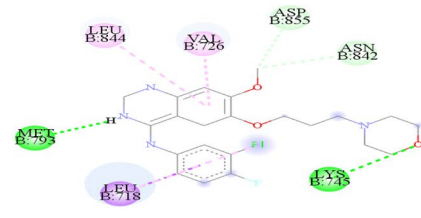
**C**  EGCG

**(ix)**



**(x)**

Binding Energy = −7.6 kcal/mol    RMSD = 0.137Å

Gefitinib

**(xi)**



**(xii)**

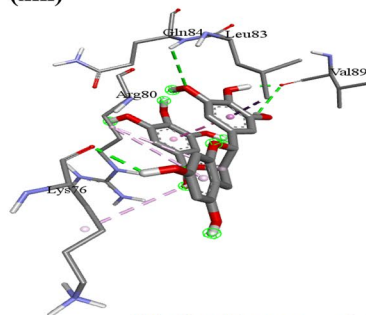Binding Energy = −7.9 kcal/mol    RMSD = 1.909Å
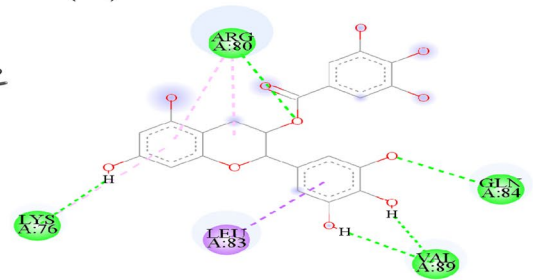
**Interactions**
- Carbon Hydrogen Bond
- Pi-Sigma
- Conventional Hydrogen Bond
- Alkyl
- Pi-Alkyl
- Pi-Cation
- Pi-Pi Stacked

**D**  EGCG

**(xiii)**
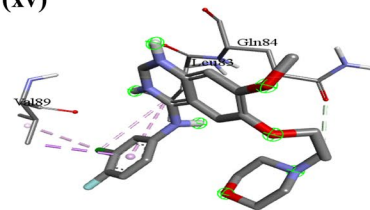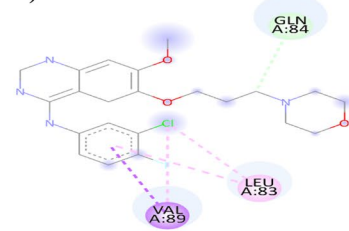


**(xiv)**

Binding Energy = −5.5 kcal/mol    RMSD = 0.149Å

Gefitinib

**(xv)**



**(xvi)**

Binding Energy = −4.6 kcal/mol   RMSD = 1.842Å

**Interactions**
- Carbon Hydrogen Bond
- Pi-Sigma
- Conventional Hydrogen Bond
- Alkyl
- Pi-Alkyl

**Table 1** The drug-likeness properties for EGCG and gefitinib listed indicate EGCG as promising lead molecule

**EGCG**

| Property | Value |
| --- | --- |
| Molecular weight | 458.38 |
| $AlogP$ | 2.23 |
| H-bond acceptor | 11 |
| H-bond donor | 8 |
| Rotatable bonds | 3 |

**Gefitinib**

| Property | Value |
| --- | --- |
| Molecular weight | 446.91 |
| $AlogP$ | 4.28 |
| H-bond acceptor | 7 |
| H-bond donor | 1 |
| Rotatable bonds | 8 |

was strongly bonded with the TKRU (BE = −7.9 kcal/mol; RMSD = 1.909 Å). The gefitinib interacted with the residues LYS745 and MET793 using a conventional hydrogen bond. Likewise, the VAL726, LEU844, and LEU718 were bonded with the gefitinib by using pi alkyl, alkyl, and pi-sigma bonds. Also, the two carbon–hydrogen bonds were formed with the residues ASN842 and ASP855 (Fig. 4C).

The EGCG interacted strongly with the transmembrane juxta membrane (TMJM) while compare with the gefitinib and formed the four conventional hydrogen bonds with the residues LYS76, ARG80, GLN84, and VAL89. Also, the BE of EGCG with the TMJM was observed as −5.5 kcal/mol with the RMSD 0.149 Å. The gefitinib interacted with the TMJM and the BE was observed as −4.6 kcal/mol with the RMSD of 1.842 Å. In that, the residues such as LEU83, GLN84*, and VAL89 use the pi alkyl, carbon–hydrogen, and pi sigma bond (Fig. 4D).

## Discussion

The present study used two cell lines to evaluate the efficacy of EGCG in inhibiting the actions of EGF viz., HPV positive ME180 and HPV negative C33A cells. EGCG treatment under basal and EGF stimulated conditions induced apoptotic changes in the morphology of the cells such as cell volume shrinkage. This could be attributed by the ability of EGCG to create an acidic ambience in the cytosol and trigger the release of cathepsin from lysosome [27]. Among the four widely used HPV cell types, ME180 cells are known to express higher levels of EGFR. We found that EGF effects are more pronounced in ME180 cells than C33A as the ability to induce migration and clone formation are greater in ME180 cells. Wound closure by EGF in ME180 cells is much faster than C33A cells. These findings indicate that EGF micro-environment could promote enhanced EMT, migration and clones in HPV positive cells. Interestingly, EGCG effects are observed in both the cell lines tested.

Extracellular matrix serves as a reservoir for growth factor and is known to prevent the effects of various drugs. They constitute collagen, proteoglycans, elastin, fibronectin and laminin. To understand the relevance of EGF on the matrix accumulation, we performed sirius red staining and alcian blue staining to visualize and quantify the collagen and GAGs, respectively. We found increased abundance of collagen and GAGs upon EGF treatment in HPV positive and HPV negative CC cells tested. This indicates the ability of EGF to augment its signaling by increased matrix component production. To ascertain the ability of EGCG in regulating the EGF induced accumulation of matrix components, we pre-treated the cells with EGCG and evaluated the accumulation of collagen and GAGs. Interestingly, we found complete inhibition of the matrix components in EGCG administered cells. Alterations in the extracellular matrix are reported during HPV infection [28]. The increase in the abundance of collagen and GAGs observed in the present investigation after EGF administration in ME180 cells and C33A cells support an earlier clinical study wherein they have reported a link between enhanced collagen and GAG production during accelerated tumor spread [29, 30].

During metastasis, the epithelial cells covering the tissue undergo EMT which makes them migrate towards adjacent and distant organs. Further, EGCG increased the effect of cisplatin in CC cells proliferation and microtubular depolymerisation effects comparable to standard tubulin drug colchicines. EGCG interfere with the signaling cascade of events leading to angiogenesis. We employed in silico analysis to find whether EGCG can bind to the catalytic site of EGFR to understand the effects of EGCG in mediating direct or indirect interactions via other signaling mechanisms. The morphological changes after treatment with EGCG indicate the absence of EMT in cells treated with EGF. Spherical shape is retained with minor cellular perturbations and did not become spindle in cells pretreated with EGCG and subsequent EGF stimulation. To explore the relevance of EMT on migration, wound healing assay was performed. EGCG pre-treatment prevented the EGF induced migration which was associated with the enzymatic activities of MMP-2 as assessed by gelatin zymography in both the cell lines tested, irrespective of HPV status. RT-PCR analysis revealed the regulatory role of EGCG in EGF induced MMP-2 gene expression.

To the best of existing information, the present study is the first to report the preventive effect of EGCG on EGF

induced EMT and migration in CC cells. Previous studies performed indicate an increase in E-Cadherin by EGCG through increase in the expression of PTEN and attenuation of PI3K/AKT signaling [31]. Induction of EMT by EGF in ME180 cells were reported to be mediated through ERK1/2 phosphorylation [3]. EGCG is known to prevent ERK/ATF2 phosphorylation in CC cells [32]. A direct evidence for the inhibitory actions of EGCG on ERK1/2 and AKT kinase in CC cells were reported by Sah et al. [32]. Further, this study reported the significance of EGCG in preventing the migration of CC cells. The observed changes in the gene expression of MMP-2 after EGF and EGCG treatment could involve the direct kinase inhibitory actions of ERK1/2. Entry of HPV has been shown to trigger EGF responsiveness in CC cells [33]. Our studies are consistent with the previous observation wherein EGCG prevented the growth factor induced phosphorylation of EGFR in YCUH891 and YCUN861 cells. These effects were associated with reduction in cyclin D1 promoter activity and reduced cell numbers and survival fraction [34]. By reducing the downstream substrate phosphorylation or inhibiting AKT activation, EGCG inhibit EGF dependent signaling pathway and abrogate HeLa cell proliferation [32]. Thus, the binding potency of EGCG with EGFR is the crucial reason for inhibiting the EGF driven migration. The drug likeness properties as evaluated by computational tools (Table 1) indicate better scores than approved EGFR TKI gefitinib, which prompts extending the present study to CDX model with HPV positive ME180 cells. The ability of EGCG in blocking the EGFR phosphorylation and other signaling molecules might provide a brief understanding on the molecular insights of newer EGCG based CC therapeutics.

## Conclusion

It appears that the effects of EGF are more pronounced in HPV positive ME180 cells and the receptivity towards EGF is more predominant in ME180 cells when compared with HPV negative C33A cells. EGCG was able to attenuate the actions of EGF in both the cell lines tested. Though a number of studies indicate a key role for EGCG in the treatment of CC, to the best of existing information, this is the first study to show the inhibitory efficacy of EGCG to prevent EGF induced matrix deposition, migration and clonogenesis in HPV positive and HPV negative CC cells. The ability of EGCG to prevent the stemness of cancer cells in the EGF TME indicates its potential utility during stem cell driven relapse conditions. Thus, EGCG has the ability to attenuate EGF driven migration of CC stem cells. Further studies are warranted to understand the role of EGCG in a

pre-clinical model system which is currently being pursued in our laboratory.

**Author contributions** Conceiving of idea, methodology, experimental design, fund acquisition and manuscript revision—SM; execution of cell based experiments, initial manuscript draft—RS, BM, SK and JG.

**Data availability** Data generated during this study will be made available from the corresponding author upon reasonable request.

## Declarations

**Conflict of interest** The authors declare no conflicts of interest.

## References

1. Muthusami S, Sabanayagam R, Periyasamy L, Muruganantham B, Park WY. A review on the role of epidermal growth factor signaling in the development, progression and treatment of cervical cancer. Int J Biol Macromol. 2022;194:179–87. https://doi.org/10.1016/j.ijbiomac.2021.11.117.

2. Hugo de Almeida V, Guimarães IDS, Almendra LR, Rondon AMR, Tilli TM, de Melo AC, Sternberg C, Monteiro RQ. Positive crosstalk between EGFR and the TF-PAR2 pathway mediates resistance to cisplatin and poor survival in cervical cancer. Oncotarget. 2018;9(55):30594–609. https://doi.org/10.18632/oncotarget.25748.

3. Muthusami S, Prabakaran DS, Yu JR, Park WY. EGF-induced expression of Fused Toes Homolog (FTS) facilitates epithelial–mesenchymal transition and promotes cell migration in ME180 cervical cancer cells. Cancer Lett. 2014;351(2):252–9. https://doi.org/10.1016/j.canlet.2014.06.007.

4. Thomas R, Weihua Z. Rethink of EGFR in cancer with its kinase independent function on board. Front Oncol. 2019;9:800. https://doi.org/10.3389/fonc.2019.00800.

5. Cai WQ, Zeng LS, Wang LF, Wang YY, Cheng JT, Zhang Y, Han ZW, Zhou Y, Huang SL, Wang XW, Peng XC, Xiang Y, Ma Z, Cui SZ, Xin HW. The latest battles between EGFR monoclonal antibodies and resistant tumor cells. Front Oncol. 2020;10:1249. https://doi.org/10.3389/fonc.2020.01249.

6. Zou C, Liu H, Feugang JM, Hao Z, Chow HH, Garcia F. Green tea compound in chemoprevention of cervical cancer. Int J Gynecol Cancer. 2010;20(4):617–24. https://doi.org/10.1111/IGC.0b013e3181c7ca5c.

7. Butler LM, Wu AH. Green and black tea in relation to gynecologic cancers. Mol Nutr Food Res. 2011;55(6):931–40. https://doi.org/10.1002/mnfr.201100058. (**Epub 19 May 2011**).

8. Tornesello ML, Annunziata C, Tornesello AL, Buonaguro L, Buonaguro FM. Human oncoviruses and p53 tumor suppressor pathway deregulation at the origin of human cancers. Cancers (Basel). 2018;10(7):213.

9. Muthusami S, Prabakaran DS, An Z, Yu JR, Park WY. EGCG suppresses Fused Toes Homolog protein through p53 in cervical cancer cells. Mol Biol Rep. 2013;40(10):5587–96. https://doi.org/10.1007/s11033-013-2660-x.

10. Periyasamy L, Murugantham B, Sundararaj R, Krishnamoorthy S, Muthusami S. Screening of MMP-2 inhibiting phytoconstituents for the development of newer pancreatic cancer modalities. Protein Pept Lett. 2023;30(4):304–13. https://doi.org/10.2174/0929866530666230213113835.

11. Shoaib S, Islam N, Yusuf N. Phytocompounds from the medicinal and dietary plants: multi-target agents for cervical cancer prevention and therapy. Curr Med Chem. 2022;29(26):4481–506. https://doi.org/10.2174/0929867329666220301114251.

12. Kilic U, Sahin K, Tuzcu M, Basak N, Orhan C, Elibol-Can B, Kilic E, Sahin F, Kucuk O. Enhancement of Cisplatin sensitivity in human cervical cancer: epigallocatechin-3-gallate. Front Nutr. 2015;1:28. https://doi.org/10.3389/fnut.2014.00028.

13. Panji M, Behmard V, Zare Z, Malekpour M, Nejadbiglari H, Yavari S, Nayerpour Dizaj T, Safaeian A, Maleki N, Abbasi M, Abazari O, Shabanzadeh M, Khanicheragh P. Suppressing effects of green tea extract and Epigallocatechin-3-gallate (EGCG) on TGF-β-induced epithelial-to-mesenchymal transition via ROS/Smad signaling in human cervical cancer cells. Gene. 2021;794:145774. https://doi.org/10.1016/j.gene.2021.145774.

14. Wang W, Xu B, Xuan H, Ge Y, Wang Y, Wang L, Huang J, Fu W, Michie SA, Dalman RL. Hypoxia-inducible factor 1 in clinical and experimental aortic aneurysm disease. J Vasc Surg. 2018;68(5):1538–50.e2. https://doi.org/10.1016/j.jvs.2017.09.030.

15. Zhu Y, Huang Y, Liu M, Yan Q, Zhao W, Yang P, Gao Q, Wei J, Zhao W, Ma L. Epigallocatechin gallate inhibits cell growth and regulates miRNA expression in cervical carcinoma cell lines infected with different high-risk human papillomavirus subtypes. Exp Ther Med. 2019;17(3):1742–8. https://doi.org/10.3892/etm.2018.7131.

16. Fullár A, Dudás J, Oláh L, Hollósi P, Papp Z, Sobel G, Karászi K, Paku S, Baghy K, Kovalszky I. Remodeling of extracellular matrix by normal and tumor-associated fibroblasts promotes cervical cancer progression. BMC Cancer. 2015;15:256. https://doi.org/10.1186/s12885-015-1272-3.

17. Cruz L, Meyers C. Differential dependence on host cell glycosaminoglycans for infection of epithelial cells by high-risk HPV types. PLoS ONE. 2013;8(7):e68379. https://doi.org/10.1371/journal.pone.0068379.

18. Liu S, Liao G, Li G. Regulatory effects of COL1A1 on apoptosis induced by radiation in cervical cancer cells. Cancer Cell Int. 2017;17:73. https://doi.org/10.1186/s12935-017-0443-5.

19. Li Q, Wang Q, Zhang Q, Zhang J, Zhang J. Collagen prolyl 4-hydroxylase 2 predicts worse prognosis and promotes glycolysis in cervical cancer. Am J Transl Res. 2019;11(11):6938–51.

20. Chen W, Huang S, Shi K, Yi L, Liu Y, Liu W. Prognostic role of matrix metalloproteinases in cervical cancer: a meta-analysis. Cancer Control. 2021. https://doi.org/10.1177/10732748211033743.

21. Mitra A, Chakrabarti J, Chattopadhyay N, Chatterjee A. Membrane-associated MMP-2 in human cervical cancer. J Environ Pathol Toxicol Oncol. 2003;22(2):93–100. https://doi.org/10.1615/jenvpathtoxoncol.v22.i2.20.

22. Muthusami S, Senthilkumar K, Vignesh C, Ilangovan R, Stanley J, Selvamurugan N, Srinivasan N. Effects of *Cissus quadrangularis* on the proliferation, differentiation and matrix mineralization of human osteoblast like SaOS-2 cells. J Cell Biochem. 2011;112(4):1035–45. https://doi.org/10.1002/jcb.23016.

23. Periyasamy L, Murugantham B, Muthusami S. Plumbagin binds to epidermal growth factor receptor and mitigate the effects of epidermal growth factor micro-environment in PANC-1 cells. Med Oncol. 2023;40(7):184. https://doi.org/10.1007/s12032-023-02048-z.

24. Krishnan A, Muthusami S, Periyasamy L, Stanley JA, Gopalakrishnan V, Ramachandran I. Effect of DHT-induced hyperandrogenism on the pro-inflammatory cytokines in a rat model of polycystic ovary morphology. Medicina (Kaunas). 2020;56(3):100. https://doi.org/10.3390/medicina56030100.

25. Periyasamy L, Muruganantham B, Deivasigamani M, Lakshmanan H, Muthusami S. Acetogenin extracted from *Annona muricata* prevented the actions of EGF in PA-1 ovarian cancer cells. Protein Pept Lett. 2021;28(3):304–14. https://doi.org/10.2174/0929866527666200916141730.

26. Sharma C, Qel-A N, Begum S, Javed E, Rizvi TA, Hussain A. (−)-Epigallocatechin-3-gallate induces apoptosis and inhibits invasion and migration of human cervical cancer cells. Asian Pac J Cancer Prev. 2012;13(9):4815–22. https://doi.org/10.7314/apjcp.2012.13.9.4815.

27. Wang L, Wei Y, Fang W, Lu C, Chen J, Cui G, Diao H. Cetuximab enhanced the cytotoxic activity of immune cells during treatment of colorectal cancer. Cell Physiol Biochem. 2017;44(3):1038–50. https://doi.org/10.1159/000485404.

28. Yuan Y, Cai X, Shen F, Ma F. HPV post-infection microenvironment and cervical cancer. Cancer Lett. 2021;497:243–54. https://doi.org/10.1016/j.canlet.2020.10.034.

29. Herbster S, Paladino A, de Freitas S, Boccardo E. Alterations in the expression and activity of extracellular matrix components in HPV-associated infections and diseases. Clinics (Sao Paulo). 2018;73(Suppl 1):e551s. https://doi.org/10.6061/clinics/2018/e551s.

30. Thangavelu PU, Krenács T, Dray E, Duijf PH. In epithelial cancers, aberrant COL17A1 promoter methylation predicts its misexpression and increased invasion. Clin Epigenet. 2016;8:120. https://doi.org/10.1186/s13148-016-0290-6.

31. Yang N, Zhang H, Cai X, Shang Y. Epigallocatechin-3-gallate inhibits inflammation and epithelial–mesenchymal transition through the PI3K/AKT pathway via upregulation of PTEN in asthma. Int J Mol Med. 2017;41(2):818–28. https://doi.org/10.3892/ijmm.2017.3292.

32. Sah JF, Balasubramanian S, Eckert RL, Rorke EA. Epigallocatechin-3-gallate inhibits epidermal growth factor receptor signaling pathway. Evidence for direct inhibition of ERK1/2 and AKT kinases. J Biol Chem. 2004;279(13):12755–62. https://doi.org/10.1074/jbc.M312333200.

33. Sizemore N, Rorke EA. Human papillomavirus 16 immortalization of normal human ectocervical epithelial cells alters retinoic acid regulation of cell growth and epidermal growth factor receptor expression. Cancer Res. 1993;53(19):4511–7.

34. Masuda M, Suzui M, Yasumatu R, Nakashima T, Kuratomi Y, Azuma K, Tomita K, Komiyama S, Weinstein IB. Constitutive activation of signal transducers and activators of transcription 3 correlates with cyclin D1 overexpression and may provide a novel prognostic marker in head and neck squamous cell carcinoma. Cancer Res. 2002;62(12):3351–5.